MODELING VISCOELASTIC RESPONSES OF THE
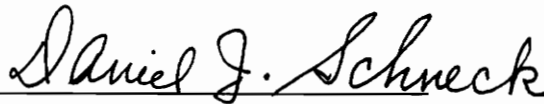# HEAD/NECK SYSTEM DURING PILOT EJECTION

by

Christopher R. Deuel

Thesis submitted to the Faculty of the

Virginia Polytechnic Institute and State University

in partial fulfillment of the requirements for the degree of

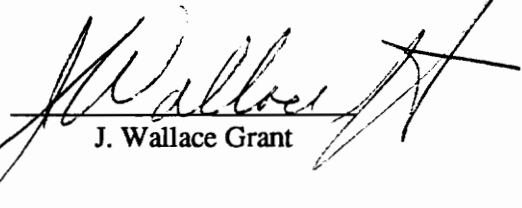## MASTER OF SCIENCE

in

Engineering Mechanics

APPROVED:

Daniel J. Schneck
Daniel J. Schneck, Chairman

Edmund G. Henneke   _J. Wallace Grant_
Edmund G. Henneke   J. Wallace Grant

May, 1994

Blacksburg, Virginia

MODELING VISCOELASTIC RESPONSES OF THE HEAD/NECK SYSTEM DURING PILOT EJECTION

by

Christopher R. Deuel

Committee Chairman: Daniel J. Schneck

(ABSTRACT)

The effect of added head mass during pilot ejection from an aircraft is currently being studied at the Wright Patterson Air Force Base in Ohio. The Articulated Total Body model, a FORTRAN computer program capable of simulating three dimensional human body motion using rigid body dynamics, has been chosen to simulate the response of the head and neck to an ejection-like acceleration. The present viscoelastic configuration of the head/neck model, which is capable of head rotation and axial neck deformation, was validated with experimental head acceleration data from live human volunteers subjected to a $10G_z$ deceleration in the Vertical Deceleration Tower at Wright Patterson Air Force Base. Experimental head z-direction acceleration data from a first subject, L7, was reproduced accurately using the ATB model. However, simulated head z-direction acceleration profiles for a second subject, B9, could not match experimental data for this subject, even after numerous variations of parameters controlling the head/neck response of the ATB model. Two of these parameters were determined to be time-varying for subject B9, and regression equations were developed describing the parameters as functions of time. Because the current ATB program does not allow time-varying parameters, the program code was modified to include two new subroutines in which the values of the parameters

are calculated with each time increment. Modifications to the ATB model resulted in an improved simulated head z-direction acceleration profile for subject B9 when compared with previous simulations using constant value parameters.

Table of Contents

List of Figures

List of Tables

1.0 INTRODUCTION

The integration of mission enhancing devices into the helmets of aircraft pilots is believed to increase the potential for head/neck injuries and fatalities during ejection(14). Additional devices such as helmet mounted displays and night vision goggles (NVG) result in increased head mass and altered center of gravity, placing possibly dangerous levels of stress on the neck. U.S. Navy statistics show that between the years of 1968 and 1988, 1.67% of ejections resulted in cervical fractures, while another 12.16% resulted in paracervical sprains and strains(4). Evaluating the response of the head and neck during an ejection allows the determination of neck loads and probability of injury; this information may then be used by engineers in the design of new helmets and safety systems.

In an effort to quantify the effects of added head mass during ejections, the United States Air Force developed a program at Armstrong Laboratory, located at the Wright Patterson Air Force base, Ohio, which is intended to evaluate the response of the human head and neck to buttocks-driven accelerations when head mass and mass distribution are altered by the addition of NVG/helmet combinations(4). Studies involve spinal-axis impact testing

with volunteer human subjects and manikins, and the use of a computer model to predict resulting head accelerations.

It is often necessary to develop a computer model of a physical process in order to calculate data which would otherwise have to be measured under adverse experimental conditions. In the case of ejection from an aircraft, a computer simulation is preferred because an experiment would involve a certain amount of risk and could not accurately duplicate the actual process in a laboratory setting. A computer simulation also greatly reduces the amount of time and expense involved in an experimental program. The computer model chosen by the Air Force is a FORTRAN program known as the Articulated Total Body (ATB) model developed by the Calspan Corporation. It is a modified version of the Crash Victim Simulation (CVS) program developed for the Department of Transportation by the Calspan Corporation to study the three-dimensional contact force environment and dynamics of a motor vehicle crash victim(4). Original modifications included the addition of aerodynamic force application and harness belt capability in 1975, while the current ATB model known as ATB-IV is capable of simulating aircraft ejection with wind blast exposure(1). In an attempt to validate the ATB model, an experiment involving nine male military personnel was conducted in which each subject was exposed to a spinal-axis 10G deceleration in the

Vertical Deceleration Drop Tower at Armstrong Laboratory. While smaller in magnitude, the 10G deceleration produces similar acceleration characteristics to that of an ACES II ejection seat. The resulting head acceleration profiles (acceleration versus time) were then compared to those obtained from simulations using the ATB program. The experiments conducted at Armstrong Laboratory and previous simulations performed using the ATB program are important to the work involved in this thesis and are described in detail in the following chapters.

The ATB program represents each portion of the human body as a rigid segment, with up to a total of 30 segments, each connected by a single joint. Included in the program is the option of representing each joint as a pin joint, ball and socket joint, globalgraphic joint, Euler joint, or a slip joint. A spring and damper may also be used with the slip joint, which allows linear translation.

Initially, the head, neck, and torso were represented as three distinct segments connected by two ball and socket joints(4). The experimentally determined values of head acceleration in the z direction for a subject, L7, were compared with simulated results using the ATB model. The acceleration profiles of the head in the x and y directions were not considered, because the maximum resultant head response was in the z-direction. The maximum acceleration

in the z-direction was much greater than predicted by the ATB model. As a result, the ball and socket joint between the upper torso and neck was replaced by a slip joint in order to simulate axial deformation of the cervical spine, as shown in Figure 1.1. The resulting acceleration profile from the simulation accurately reproduced the head z-direction acceleration profile for subject L7.

Following Estep's work, Miller and Schneck(8) compared experimental head acceleration profiles from another subject, B9, with simulated results to further validate the ATB model. The same joint options were chosen for the head, neck, and upper torso, with a ball and socket joint between the neck and head, and a slip joint between the upper torso and neck. Initially, a good simulation could not be obtained; the ATB model was unable to match the maximum amplitude of the head z-direction acceleration. It predicted a smaller maximum amplitude occurring at a later time than measured.

Next, Miller and Schneck evaluated seven parameters affecting the biodynamic response of the head/neck model system, which are described in detail in section 4.2. These values were optimized using an iterative procedure. The new acceleration profile obtained using the optimum values for the parameters represented the experimental data more accurately, but was still unable to match the time and

4
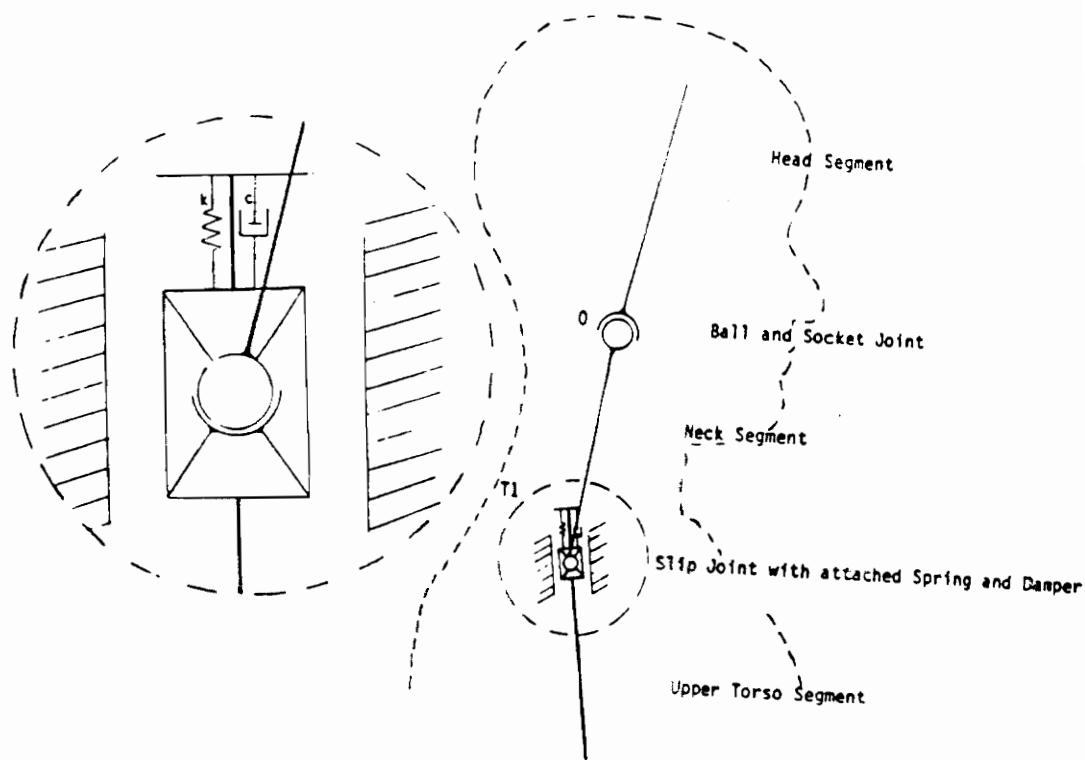
Figure 1.1 Viscoelastic Representation of the Neck/Torso Joint
Used in the ATB program[4]

amplitude of the experimental maximum acceleration.

As a result, it was suggested that the ATB model in its current form could not accurately simulate the biodynamic head/neck response during the experiment; it lacked some of the physics necessary to model the complex structure of the neck(8). Because the neck exhibits viscoelastic behavior; i.e. the response of the neck to a force depends on the rate at which it is deformed, it was proposed that the parameters affecting the response of the head/neck system are also time-dependent. The experimental head acceleration profile data was divided into four distinct time regions, and the values of the parameters were optimized for each time region.

At least two of the parameters were determined to be functions of time. The linear translational viscous coefficient of the damper, c, was found to be a linear function of time up to a certain point, t_o, while NPs1, the linear spring coefficient resisting flexure (forward head rotation) at the neck joint, was found to decrease exponentially after t_o. The present version of the ATB program does not allow any parameters to be defined as functions of time. Instead, all parameters are read from a separate input file at the beginning of the program and remain constant during its execution. It is the intent of this thesis to modify the current ATB program code to allow

c and NPs1 to be defined as functions of time at the joint between the upper torso and neck. The values of these two parameters will be updated with each time increment by introducing two new subroutines into the ATB program. Simulations using the modified ATB program will be compared with experimentally measured values of head z-direction acceleration for subject B9.

2.0 LITERATURE REVIEW

The study of biomechanics of the human head, neck and spine provides valuable information in the evaluation and prevention of spinal injuries due to external mechanical loading. This information allows engineers to develop safety systems used to prevent injury resulting from dynamic loading associated with falls, sports injuries, pilot ejections, and vehicular accidents(17). Several models have been developed to simulate the response of the spine to dynamic loading, ranging from earlier continuum, discrete, and lumped parameter models to more modern finite element models.

One of the earliest continuum models used in the study of the pilot ejection problem was developed by Hess and Lombard (17). The spine was represented as a homogeneous elastic rod, with known length, density, and modulus of elasticity, which is free at one end and subjected to an acceleration along its length at the other end, as demonstrated in Figure 2.1B. The model is considered to be a single parameter model in that the acceleration of the rod is a function of the time required for a stress wave to travel the length of the rod. The model was correlated with experimental head acceleration data obtained from the Douglass Aircraft Company. The model predicted the first
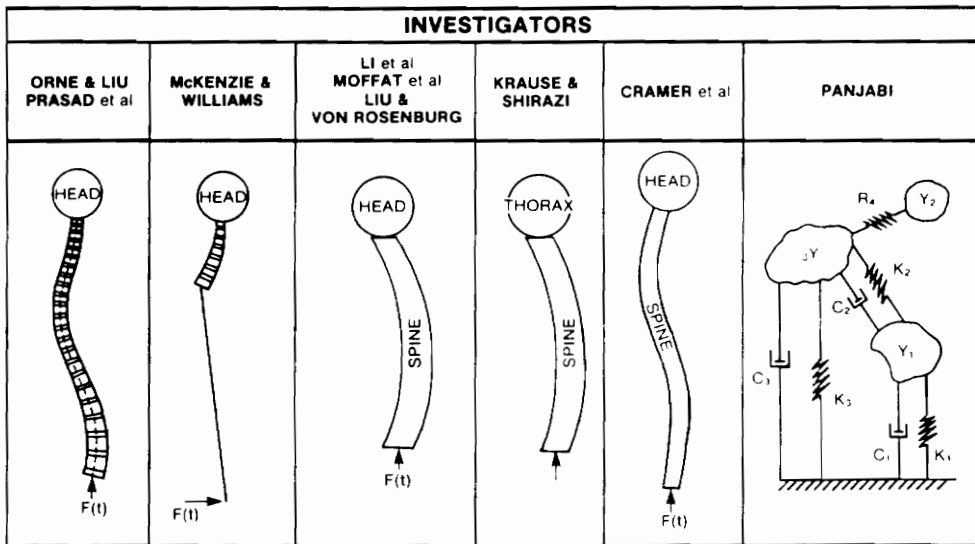
A
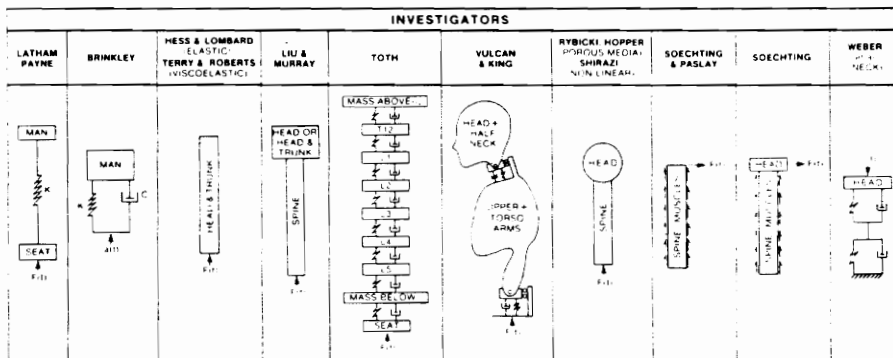
B

Figures 2.1A-B   Continuum and Lumped Parameter Models of Spinal Deformation (17)

acceleration peak of 20G's with good accuracy, but had little correlation with the remaining data. It was suggested that the lack of damping was probably the cause for the poor correlation. Several attempts were made to improve the continuum model of Hess and Lombard, including the introduction of damping, the addition of a head mass, and the modification of the spine as a curved rod(17). Several of these models are shown in Figures 2.1A and 2.1B.

The earliest use of a lumped parameter model to predict the dynamic response of the spine in a pilot ejection situation was by Latham(17). He represented the spine as a one degree of freedom system with a spring connecting two masses representing the body and ejection seat. Following Latham, Payne developed a damped spring-mass model which predicted the probability of spinal injury as a function of deflection and spring reaction force(17). This model was eventually adapted by the Air Force for use in the study of ejection seats and capsules. It was later modified to include a multi-mass spring-dashpot system, capable of predicting failure of vertebrae from T11 to L5.

Weber developed a dual spring-dashpot system representing the cervical spine for use in tensile and compressive loading, with a single mass representing the head as shown in Figure 2.1B. The model was loaded at various input velocities, and spring constants were

determined for each velocity rate by fitting analytical deflections to experimentally determined deflections(17). Weber then represented the optimum value of the spring constant in the form of a power series, with velocity as the dependent variable.

An alternative method to using mathematical models in the prediction of human response during ejection involves the use of manikins in impact testing. One of the more advanced forms of manikins, known as the Advanced Dynamic Anthropomorphic Manikin (ADAM), was developed by the Air Force for use in the testing of escape systems and various crew protection systems and procedures(5). The manikin, shown in Figure 2.2, consists of seventeen segments whose structure is based on dimensions and inertial properties obtained from a USAF male aviator anthropometric survey(15). It is capable of simulating human joint articulation, along with axial compression of the neck and spine. The spine consists of a combined spring and hydraulic damping element which allows only axial compression or extension. The neck element, based on the Hybrid III manikin cervical spine, consists of three rigid aluminum vertebral elements molded into a 75 durometer butyl elastomer and is capable of both flexion and compression(16). There are two forms of ADAM available, a small and large ADAM based on the 3rd and 97th percentile from the USAF survey.

Table 2.1 ADAM vs. Human Response[3]

CHANNEL	HUMAN MEAN	ADAM-S		ADAM-L	
		MEAN	% CHANGE	MEAN	% CHANGE
HEAD Z ACCEL (G)	11.57	11.35	NSD	15.65*	+35%
CHEST Z ACCEL (G)	13.49	13.45	NSD	17.90	+33%
CHEST X ACCEL (G)	3.70	4.01	NSD	2.62	NSD
HEAD Z ACCEL (ms)	71.1	71.0	NSD	72.9	NSD
CHEST Z ACCEL (ms)	78.1	70.8	-9%	74.6	NSD
CHEST X ACCEL (ms)	65.1	73.8	+13%	75.8	+16%
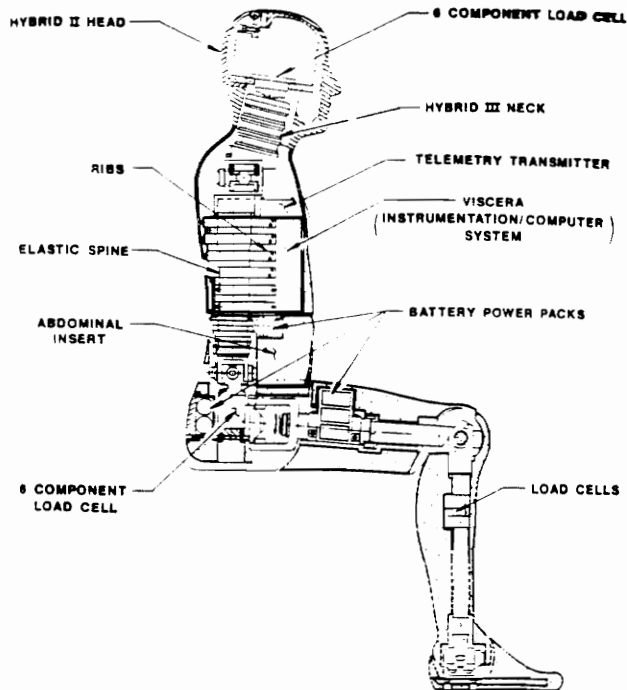
Figure 2.2   ADAM Manikin[15]

In an experiment conducted at the Armstrong Laboratory Vertical Drop Tower (VDT) facility, six small and eight large ADAM manikins were subjected to a $10G_z$ vertical deceleration(3). Resulting head and chest accelerations were recorded using internally mounted sensors. Head and chest acceleration data was then compared with data obtained from fourteen human subjects who were tested under similar conditions. A statistical comparison of the data in Table 2.1 demonstrates the ability of the small ADAM to predict peak magnitudes of human head and chest accelerations. The mean maximum head z acceleration of the small ADAM was 11.35 G's, compared with 11.57 G's for the human subjects. The mean time-to-peak acceleration measurements were nearly identical, occurring at 71.0 and 71.1 msec for the manikin and human subjects, respectively. The large ADAM, however, predicted a much greater head z-acceleration of 15.65 G's, representing a 35% difference when compared with the human response.

In an effort to evaluate the effect of helmet mounted devices on the response of the head and neck during axial impacts, a device known as the Head-Neck Pendulum (HNP) was created in order to isolate the dynamic response of the head and neck(2). The device, constructed at the Armstrong Laboratory, was intended to provide a means for accurate, repeatable and inexpensive testing. The HNP consists of a

beam connected to a frame, with an ADAM head and neck structure mounted to the base of the free end. In a study conducted at the Armstrong Laboratory, the validity of the HNP was determined by comparing head acceleration values of the HNP with values obtained from impact testing of ADAM manikins without helmets in the Vertical Deceleration Tower. The pendulum was decelerated using a spring and variable hydraulic damper, producing an input acceleration similar only in magnitude to that of the measured ADAM chest acceleration (Figure 2.2A). A comparison of the HNP head acceleration profile with the ADAM head acceleration profile in Figure 2.2B demonstrates the HNP's ability to duplicate the peak acceleration in magnitude only.

In previous work by Estep, experimental results from subject L7 (height 68.8 inches, weight 150 lbs) were chosen to validate simulations using the ATB model(4). Three different test configurations were chosen: the original ball and socket representation of the head/neck and neck/torso joints, the same configuration with added resisting torques to simulate resistance of muscles and ligaments, and a viscoelastic slip joint replacing the ball and socket joint at the neck/torso joint. Because 98.5% of the experimentally measured maximum head acceleration for subject L7 was in the positive z-direction, validation of the simulated response was based on how well the simulated
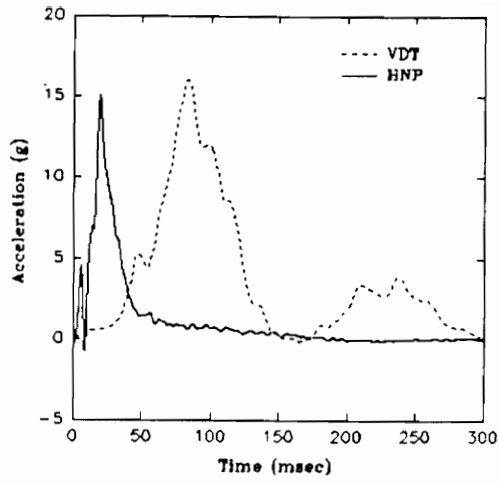
Figure 2.2A   ADAM(VDT) Chest Acceleration and Pendulum(HNP) Input
Acceleration(2)
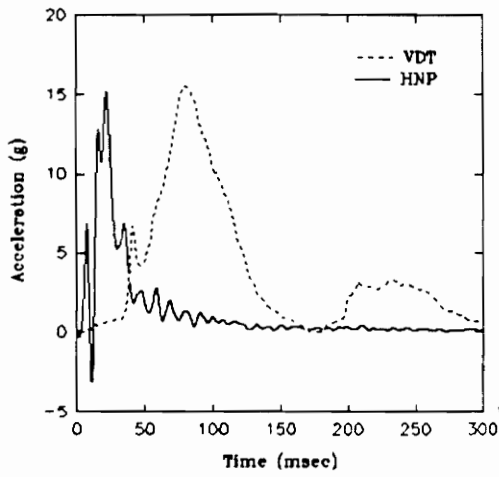
Figure 2.2B   Comparison of HNP and ADAM(VDT) Head Acceleration
Profiles(2)

15

z-direction head acceleration profile correlated with the corresponding measured head acceleration profile. Both experimental and simulated accelerations have been adjusted so that they are relative to the earth's gravitational field.

Initially, the input file to the ATB program was set up for subject L7 using a combination of measured anthropometric data and the GEBOD program. Values for flexure spring coefficients and viscous function coefficients provided by the GEBOD program, listed in Table 2.2, were used as initial approximations for both the head/neck and neck/torso joints. Simulations using the first configuration described above produced an acceleration profile with little correlation to the actual human response. An acceleration spike at approximately 140 msec was a result of complete head rotation and chin to chest contact. In order to reduce the amount of head rotation, increased values of 150 in-lb/degree for the linear spring coefficient were chosen to simulate muscle and ligament resistance for both the head/neck and neck/torso joints. The remaining coefficients were held at the same values. The modified simulation in Figure 2.3 more closely resembles the human response. However, the simulated acceleration profile fails to match the maximum measured head z-acceleration of 15.66 G's at 81 ms, with a maximum

Table 2.2 Flexure Spring Coefficients

Linear Spring Coefficient	in-lb/deg	0.0
Quadratic Spring Coefficient	in-lb/deg^2	5.0
Cubic Spring Coefficient	in-lb/deg^3	0.0
Viscous Coefficient	in-lb-sec/deg	0.1
Energy Dissipation Coefficient	dimensionless	0.7

Figure 2.3   Comparison of Experimental and Simulated Head Z-Direction
Acceleration Profiles for Subject L7 Using Ball and Socket
Configuration(4)

18

acceleration of only 12.04 G's at 76 ms. Estep was unable to increase the maximum acceleration in further simulations using this test configuration.

As a result, the neck/torso ball and socket joint was replaced with a combination of a slip joint with a spring and viscous damper to simulate axial deformation of the neck. Additionally, the possibility of head and neck rotation was eliminated by locking the joints to relative segment angular motion. Several simulations were performed using different values for the spring and damping coefficients, with best results obtained using linear and quadratic spring coefficients of 50 lb/in and 100 lb/in respectively, and a linear damping coefficient of 1.5 lb-sec/in. The simulated response closely resembles the measured response as demonstrated in Figure 2.4. The maximum head z-direction acceleration achieved was 15.01 G's at 80 ms, which is 96% of the maximum measured acceleration, compared to 77% using the previous ball and socket configuration. In addition, the time at which the maximum simulated and measured accelerations occur are nearly identical, with only one ms of phase difference. It can be seen from these results that Estep was able to produce an adequate simulation of the response of subject L7 using the ATB model.
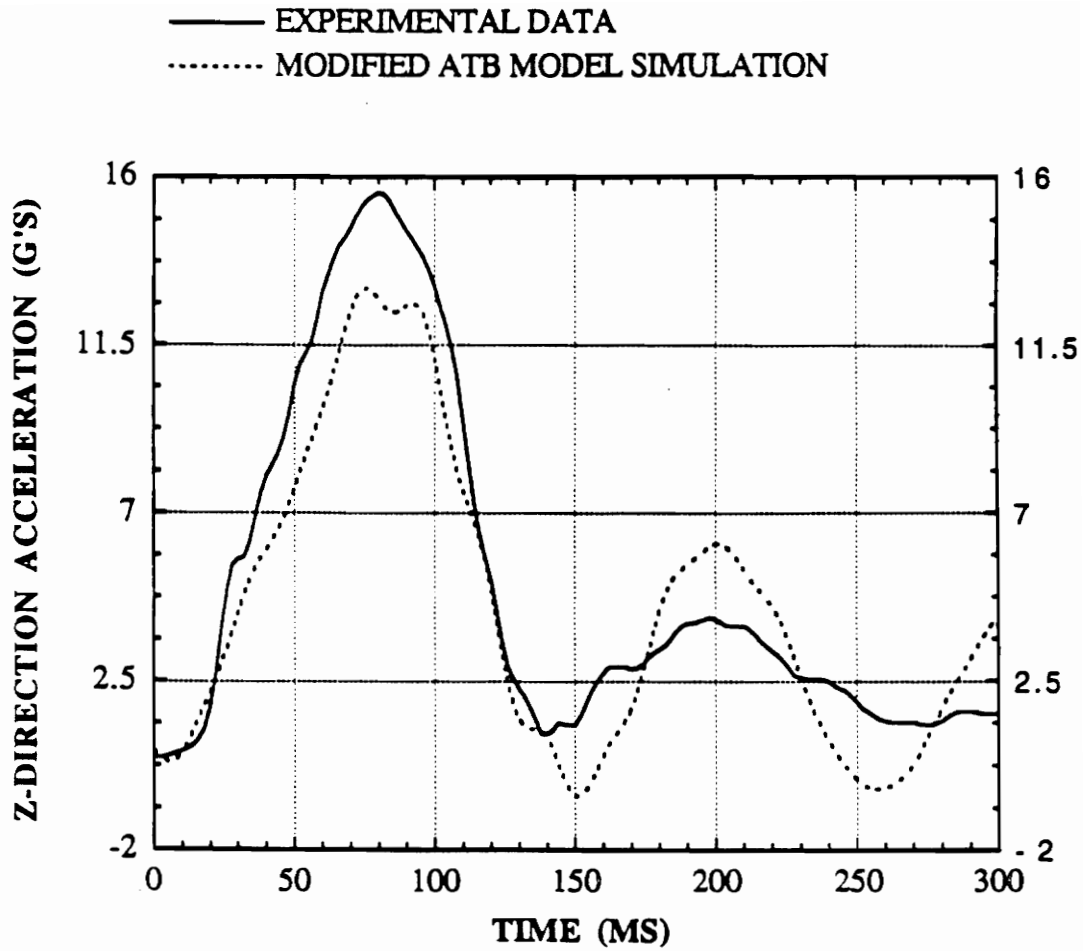
EXPERIMENTAL DATA
VISCOELASTIC MODEL SIMULATION
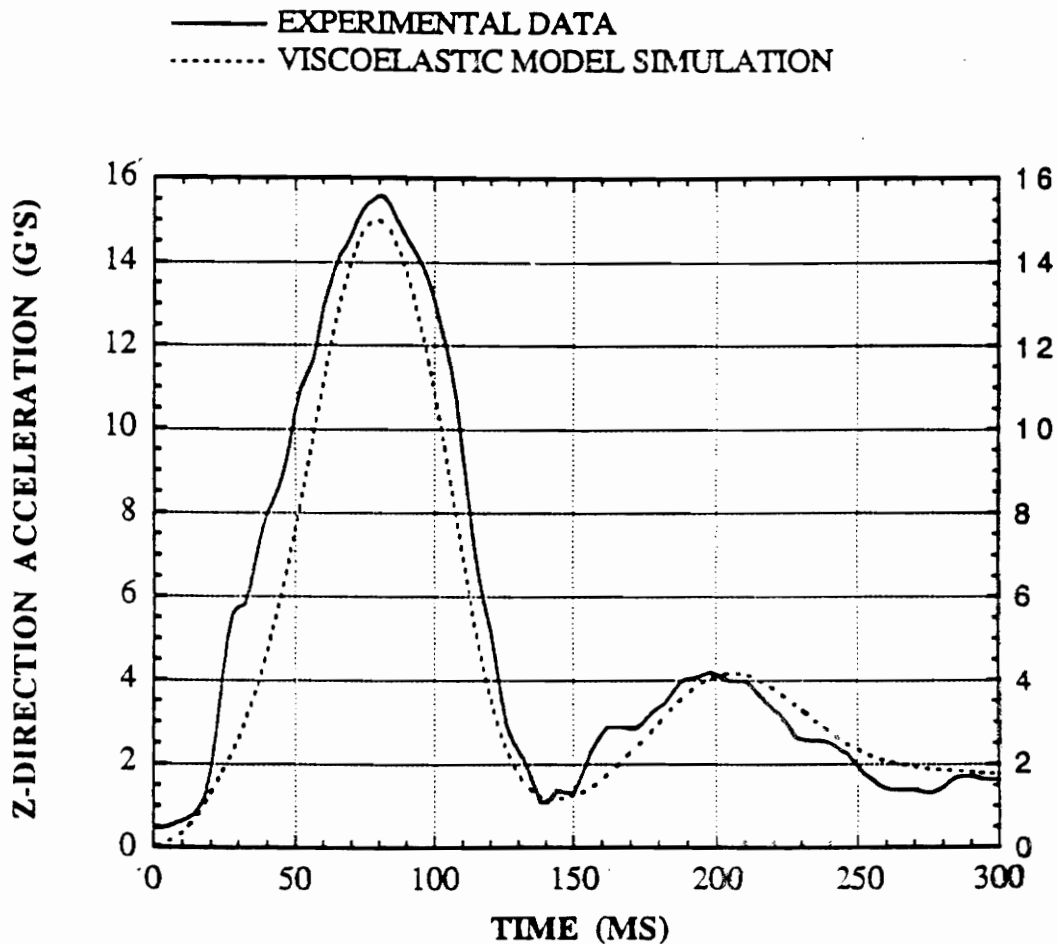
Figure 2.4 Comparison of Experimental and Simulated Head Z-Direction Acceleration Profiles for Subject L7 Using Viscoelastic Configuration(4)

3.0 OPERATION OF THE ATB PROGRAM

3.1 Mechanics of the ATB Program

The Articulated Total Body (ATB) model was developed to simulate three dimensional human body dynamics during potentially hazardous situations, such as aircraft ejections and automobile crashes(9). The body is subjected to a simulated dynamic environment consisting of applied and interactive contact forces. The ATB model is a computer driven mathematical model based on rigid body dynamics using Eulerian equations of motion with Lagrangian type constraints(5). It is unique in that it allows the total number of segments and joints used in the simulation to be varied.

The standard model configuration used in simulating ejections consists of 15 or 17 rigid body segments including the head, neck, upper torso, center torso, lower torso, upper arms, lower arms, upper legs, lower legs and feet. Each segment is connected to another segment by a single joint, resulting in a total of n segments and n-1 joints. A schematic of the 17 segment/16 joint configuration is shown in Figure 3.1. In this report a total of three segments and two joints were chosen to evaluate the response of the head and neck to a $10G_z$ impact deceleration, including the head, neck and upper torso. For each segment the structure,

21

BODY SEGMENTS

1	Lower Torso
2	Middle Torso
3	Upper Torso
4	Neck
5	Head
6	Right Upper Leg
7	Right Lower Leg
8	Right Foot
9	Left Upper Leg
10	Left Lower Leg
11	Left Foot
12	Right Upper Arm
13	Right Lower Arm
14	Right Hand
15	Left Upper Arm
16	Left Lower Arm
17	Left Hand
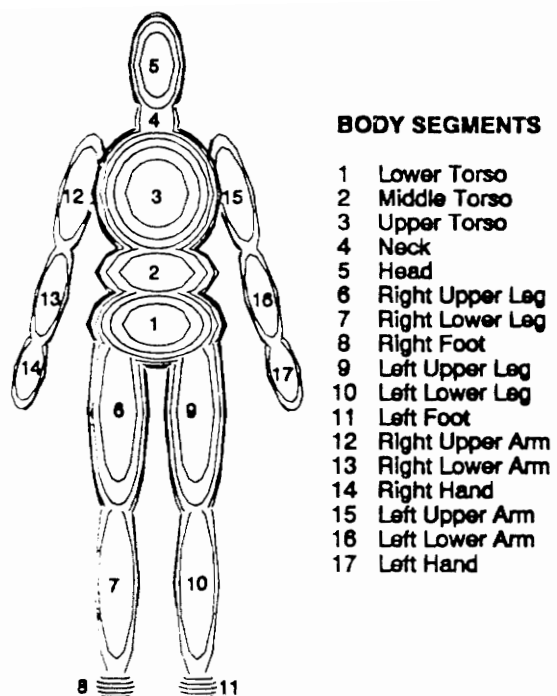
Figure 3.1   17 Segment/16 Joint ATB Configuration(9)

dynamics and relationship with the adjacent segment are considered, resulting in a prediction of the response of the complete model.

The center of mass of segment n, located at Rn, is defined with respect to an external inertial coordinate system, which can be placed at any convenient point in space as demonstrated in Figure 3.2. Principal axes of segment n, Xpn, Ypn and Zpn, originate from the center of mass and are defined with respect to the inertial coordinate system. The geometric properties of the segment are then defined using the principal axes, including the geometric center of the segment. Three ellipsoidal radii, azn, ayn, and axn, originating from the geometric center are specified and define an ellipsoidal contact surface for the segment. The contact surface is rigidly attached to the center of mass of the segment. The locations of joints within the segment are defined, and at each joint two coordinate systems rigidly attached to the connected segments are assigned with a common origin. The angular displacement of one segment with respect to the adjacent segment can then be determined, allowing the application of resistive torques as a function of torsion and flexion angles, shown in Figure 3.2.

External forces are applied to the ellipsoidal surface at the point of contact with the segment. These forces are generated from contact between segment surfaces and external
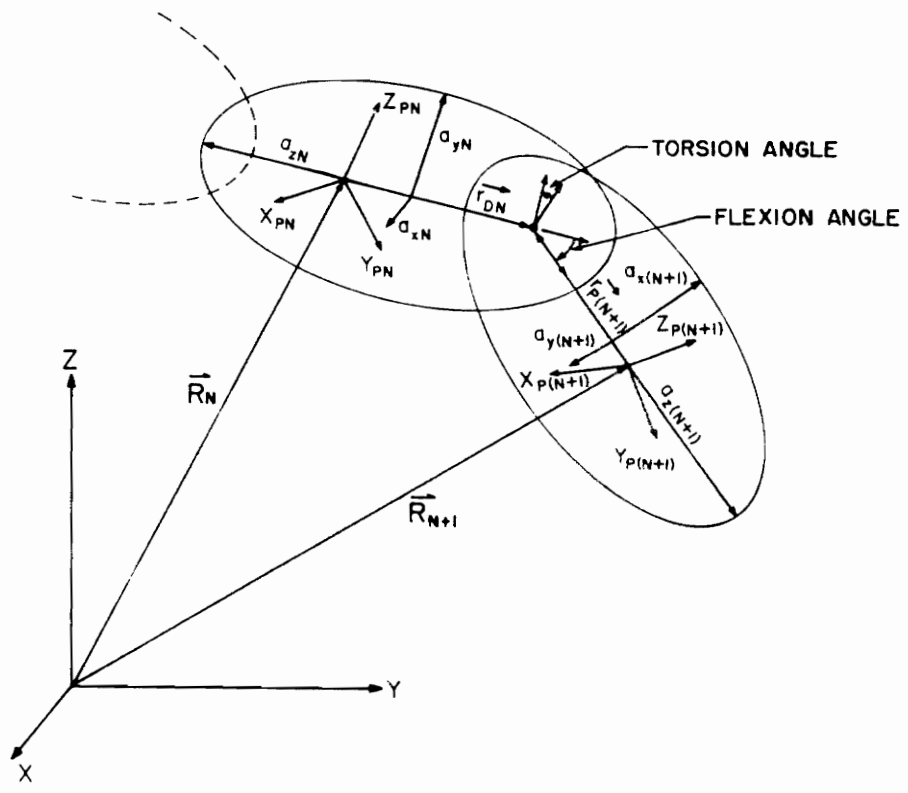
Figure 3.2   Basic Body Segment Properties and Coordinate Systems (5)

24

planes, segment to segment contact, and optional input to the program including wind forces and restraint systems. The external dynamic environment to which the body is subjected must also be included as input to the program. By considering the motion of each rigid segment to be a combination of translation and rotation, the most general system equations of motion can be defined as (4):

$$\sum \vec{F} = m\ddot{\vec{x}}$$
(3.1)

and

$$\sum \vec{N} = \dot{\vec{H}}$$
(3.2)

where

m   =   the mass of the segment

$\ddot{\vec{x}}$ =   the acceleration of the center of mass of the segment

$\sum \vec{F}$ =   the sum of applied and interactive contact forces

$\dot{\vec{H}}$ =   the rate of change of angular momentum of the segment about its center of mass

$\sum \vec{N}$ =   the sum of all torques and moments applied to the segment

The dynamic equations for each segment are combined into matrix equations, which are described in detail in reference (4).

3.2 Input to the ATB Program

Input to the ATB program consists of a formatted input file divided into nine different sections known as cards(10):

Cards A - Date and run description, units of input and output, control of restart, integrator and optional output.

Cards B - Physical characteristics of the segments and joints.

Cards C - Description of the vehicle motion.

Cards D - Contact planes, belts, air bags, contact (hyper) ellipsoids, constraints, symmetry options, spring dampers, and prescribed forces and torques.

Cards E - Functions defining force-deflections, inertial spike, energy absorption factor, and friction coefficients.

Cards F - Allowed contacts among segments, planes, belts, airbags, contact (hyper)ellipsoids and harnesses.

Cards G - Initial orientations and velocities of the segments.

Cards H - Control of output of program.

Cards I - Control information for plotter output.

Three segments were chosen to model the response of the head and neck to a $10G_z$ impact deceleration for subjects L7 and B9, consisting of the upper torso, neck, and head. The physical properties of the segments included as input to the program are the principal moments of inertia, mass, contact surface ellipsoid center and radii, joint locations and segment interaction characteristics. These properties may be obtained using a combination of anthropometric data and a program included with the ATB program known as GEBOD, or GEnerator of BOdy Data. The GEBOD program uses regression equations based on height and weight to calculate anthropometric data for adult males, females, and children (9).

Joint properties must also be specified as input to the program, including the type of joint as well as the torque properties of the joint. The various types of joints which may be chosen in the ATB program are pin joint, ball and socket joint, globalgraphic joint, Euler joint and slip joint. In addition, the initial condition of the joint may be locked or unlocked. The passive resistance of ligaments and muscles to torsion and flexion, as defined previously, is modeled by a viscous damper and non-linear spring. Two separate sets of coefficients are required to define the flexural and torsional spring characteristics.

The slip joint is the only joint which allows linear

translation between adjacent segments and may be used in combination with a Voigt model spring and damper, discussed in section 4.3. The linear and quadratic spring coefficients, along with the linear and quadratic viscous coefficients, are included as input to the program. In addition, the slip joint may be defined as having complete or limited angular freedom.

A description of the physical and dynamic properties of the vehicle containing the body must be contained in the input file, including such options as wind force and restraints. The vehicle motion may be defined in terms of position, velocity or acceleration with respect to time. The measured z-direction chest acceleration is used as input to the ATB program for subject B9, as shown in Figure 3.3.
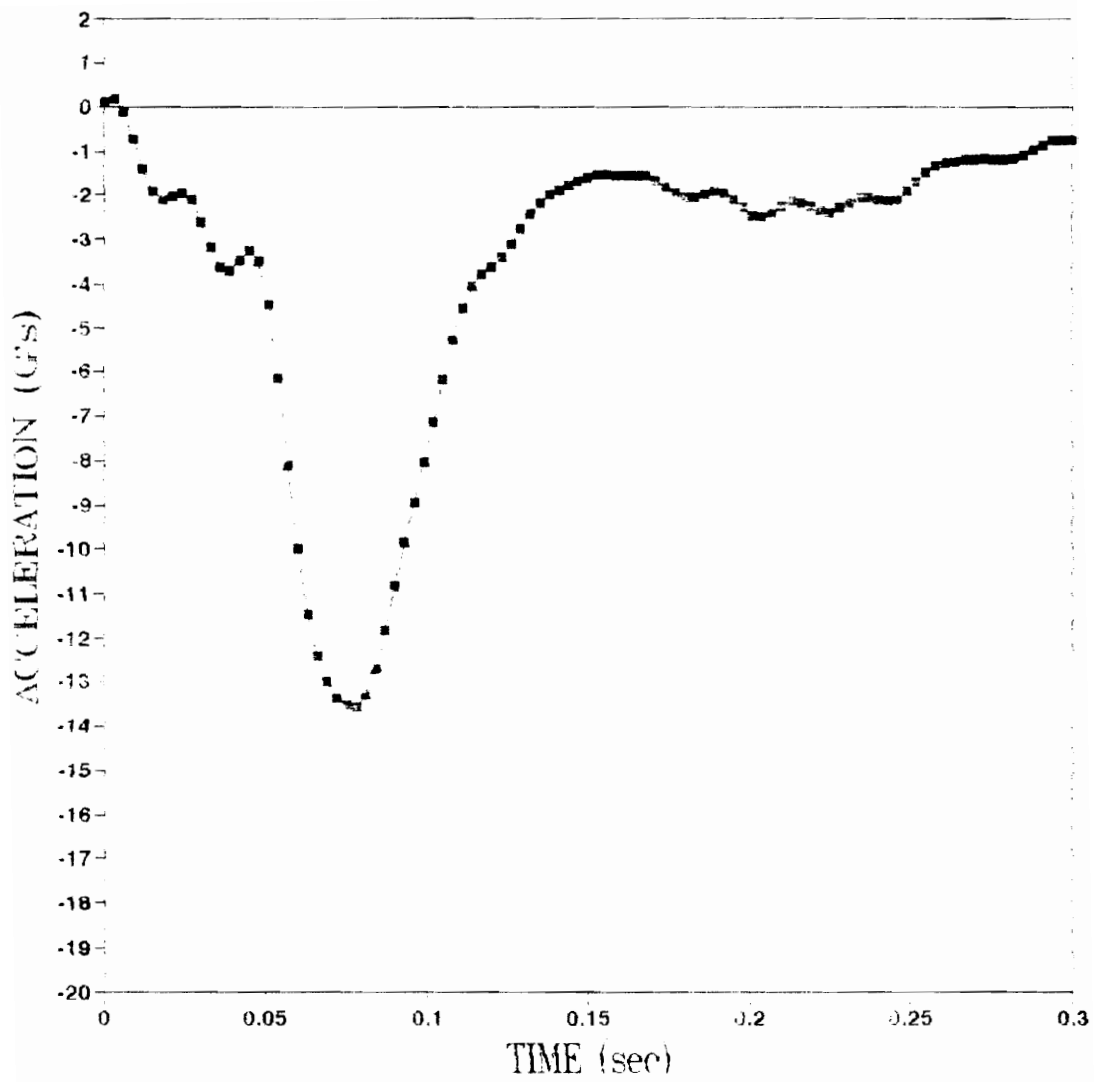
Figure 3.3 Input Acceleration to the ATB Program for Subject B9

4.0 PROBLEM STATEMENT

4.1 Experimental Data

The experimental data to which the ATB-IV model is compared was collected using the Vertical Deceleration Drop Tower at Armstrong Laboratory. Nine male military personnel participated in the experiment, which required a seated subject wearing an HGU-26/P helmet and a MBU-5/P mask(4). The test seat carriage of the Tower was allowed to free-fall within a guide rail system and then impact against a hydraulic deceleration device, resulting in a rapid deceleration of the subject. Upon impact, a plunger located under the test seat controlled the deceleration of the subject by displacing water in a filled cylinder located at the bottom of the tower. Overall, the resulting deceleration profile was determined by the initial height of the test seat, the shape of the plunger, and the diameter of the cylinder containing water. This deceleration profile is dynamically representative of an upward acceleration produced by an ejection.

The acceleration of the seat, carriage, and the head and chest of each subject were measured during the test. The test accelerometer coordinate system defined with respect to the test seat is shown in Figure 4.1. The z-axis is positive in the buttocks to head direction of the
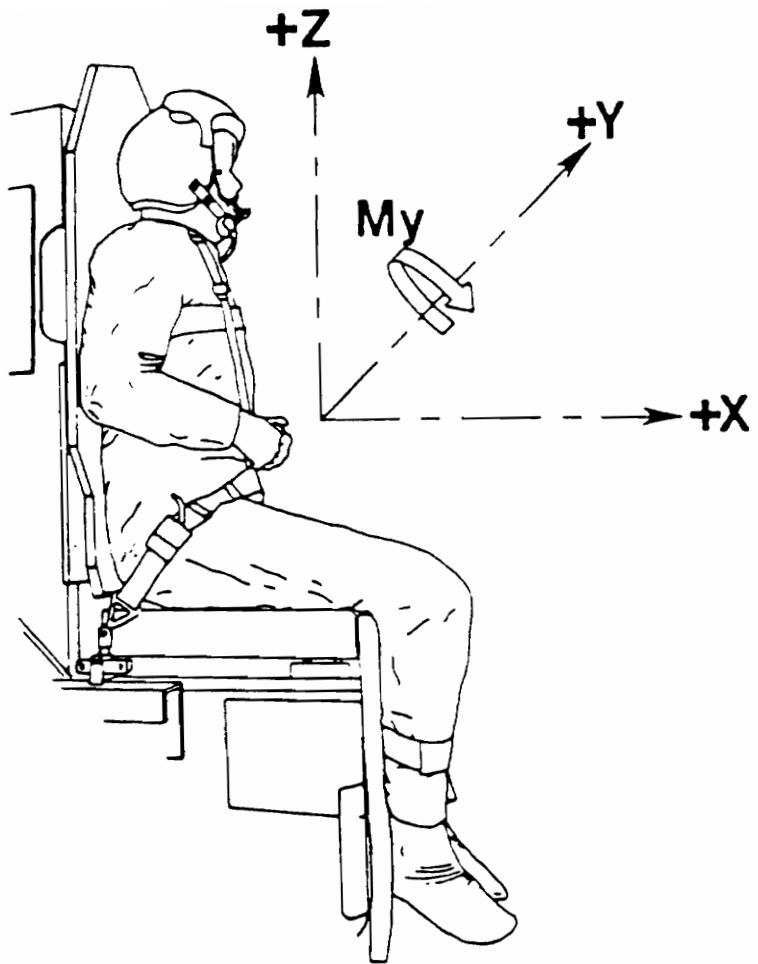
Figure 4.1 Experimental Configuration and Accelerometer Coordinate System (4)

subject, while the x-axis is positive in the direction in which the subject would be looking forward. The ATB program uses a similar coordinate system, except that the z-axis is positive in the opposite direction. The x, y, and z linear accelerations and the angular acceleration about the y axis were measured for the subject's head using a set of four accelerometers mounted to the external edge of a plastic dental bite block inserted into the mask. The same accelerations for the chest were measured using a set of four accelerometers mounted to a chest block in the area of the sternum.

The time t = 0 represents the point of impact with the deceleration device, with the previous time period representing free-fall. The resulting head accelerations for subject L7 are shown in Figure 4.2. It was determined that 98.5% of the subject head maximum resultant response acceleration was in the z-direction, and that head rotation is minimally involved in the response mechanism for the head and neck when a subject is exposed to a $10G_z$ deceleration.

The head acceleration profiles for subject B9 are shown in Figures 4.3A-D. The maximum value of the z-direction head acceleration, 18.32 G's, represents 99.8% of the maximum resultant head acceleration of 18.35 G's at 72 msec. The maximum head acceleration in the x direction was measured as -2.76 G's at 51 msec, while the maximum
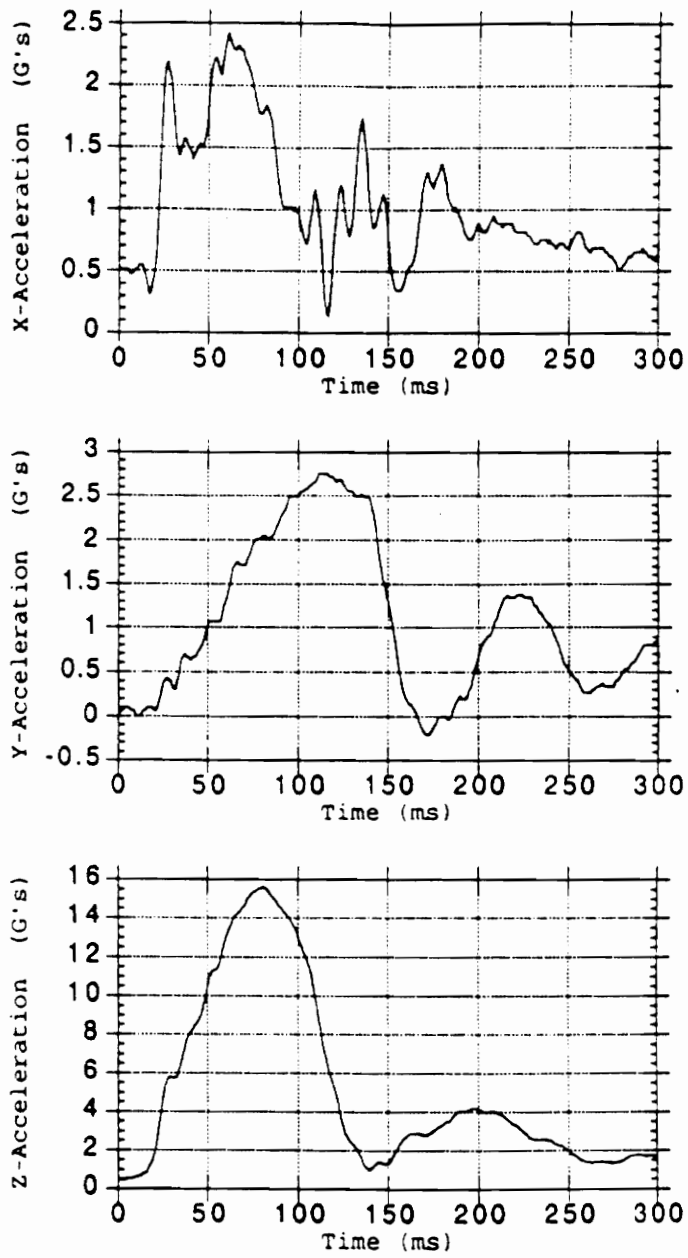
Figure 4.2   Measured Head Acceleration Profiles for Subject L7(4)
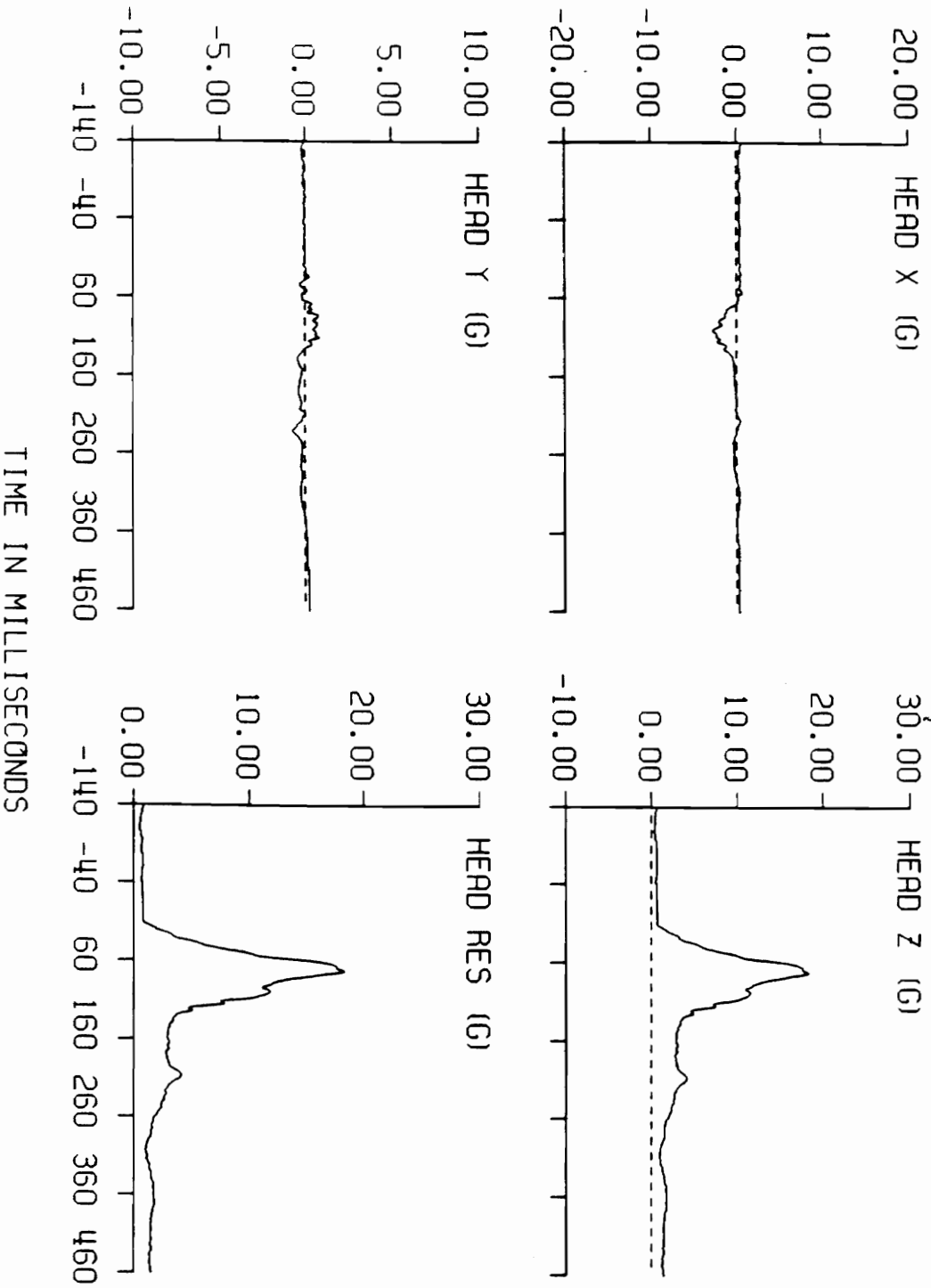
Figure 4.3   Measured Head Acceleration Profiles for Subject B9

34

acceleration measured in the y-direction was 0.85 G's at 111 msec.

4.2 Validation of Subject B9

In additional studies using the ATB model, Miller chose head acceleration data from subject B9 (height 69.0 inches, weight 147 lbs) to further validate simulated head acceleration profiles(8). Subject B9 was chosen because of the time and magnitude of peak head acceleration, which represent extreme values when compared with those of other subjects. The ball and socket head/neck joint and viscoelastic neck/torso joint configurations were maintained, although both joints were unlocked to angular displacement as a result of a measured 10.3 degrees of forward head rotation. A total of seven parameters affecting the response of the model were chosen for evaluation. These included : 1) the head/neck joint linear flexure spring coefficient (HPs1), 2) the head/neck joint linear flexure viscous coefficient (HPv1), 3) the neck/torso joint linear flexure coefficient (NPv1), 4) the neck/torso joint linear flexure viscous coefficient (NPv1), 5) the spring/damper linear translational spring coefficient (k1), 6) the spring/damper quadratic translational spring coefficient (k2), and 7) the spring/damper linear translational viscous coefficient (c).

The primary criterion chosen for evaluating the response of the ATB model and obtaining the best possible values of the seven parameters was to be able to match the magnitude and time into the response of the measured maximum head z-acceleration. Other factors considered were the ability of the simulation to duplicate the overall head z-acceleration profile, including a small plateau occurring after the maximum acceleration. Initial values selected for the seven parameters are displayed in Table 4.1.

The ATB input file was set up for subject B9 using anthropometric data and the GEBOD program. In an attempt to determine the effect of each parameter on the acceleration profile, sets of several simulations were run in which one parameter was varied while the others were held constant. Miller concluded from these results that the spring constants affect mainly the magnitude of the response, while the viscous coefficients essentially shift the acceleration profile with respect to the time axis. Next, an iterative procedure was developed to determine the best possible values of the seven parameters.

This iteration scheme consisted of holding all but one of the seven parameters constant and varying it until no significant improvements in the simulated response could be obtained. Next, this same procedure would be performed with

Table 4.1   Initial Parameter Values For Subject B9

HPs1	in-lb/deg	100
HPv1	in-lb-sec/deg	1.0
NPs1	in-lb/deg	100
NPv1	in-lb-sec/deg	0.7
k1	lb/in	50
k2	lb/in^2	100
c	lb-sec/in	1.5

Table 4.2   Parameter Values For Subject B9
After First Iteration

HPs1	in-lb/deg	450
HPv1	in-lb-sec/deg	14.9
NPs1	in-lb/deg	880
NPv1	in-lb-sec/deg	1.0
k1	lb/in	50
k2	lb/in^2	500
c	lb-sec/in	5.6

the second parameter, holding the first parameter constant at its optimized value. This process was repeated for all seven parameters in a series of two iterations. The results of these iterations suggested that locking or unlocking the head/neck joint had little or no effect on the acceleration profile; therefore, the head/neck joint was locked. Best results were obtained using values from the first iteration listed in Table 4.2. In Figure 4.4, a comparison of the simulated response using the tabulated values with experimental results allows a good amplitude match, but the maximum amplitude of the simulated response occurs at a later time. The effects of adding non-linearity to the slip joint were considered but did not result in any improvements in the response. From these results, Miller concluded that the ATB model could not provide an adequate simulation in its present configuration.

4.3 Viscoelastic Nature of the Neck

From an anatomical, neurological, and mechanical point of view, the neck is quite complex(7). The response of the neck to an external load is primarily controlled by the mechanical properties of the cervical spine and surrounding ligaments and musculature. The viscoelastic properties of biological materials contributes to this complexity, along

Subject B9
Comparison of Experimental Data to ATB
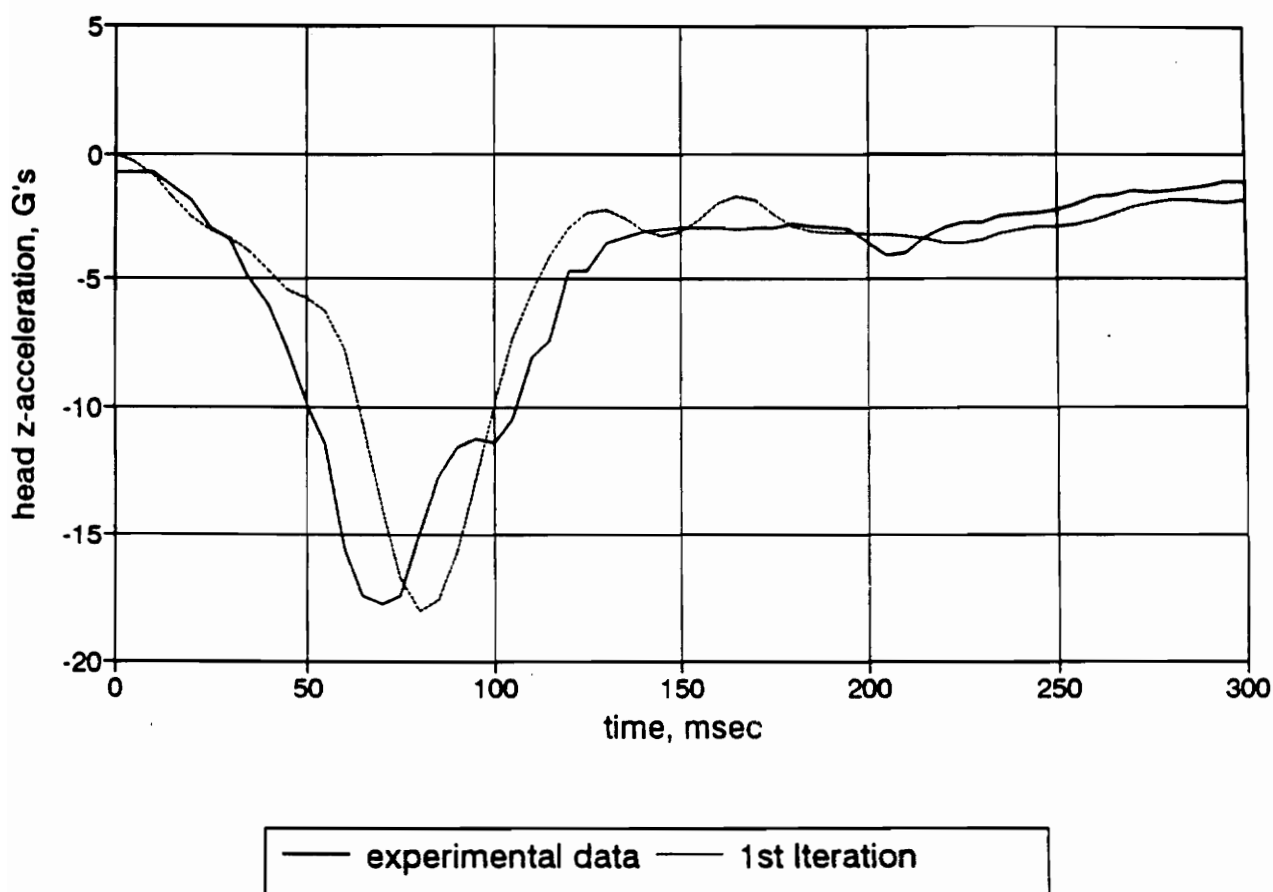
Figure 4.4   Comparison of Simulated and Experimental Head Acceleration
Profiles for Subject B9 After 1st Iteration of Parameters [8]

with the active contraction of muscles which results in changes in their mechanical properties.

In a study by McElhany, Paver, McCrackin, and Maxwell, the mechanical properties of the cervical spine were determined by evaluating the response of unembalmed human cervical spines to compression loading(7). Relaxation tests were performed by applying a ramp displacement of 0.7 cm in 25 msec, followed by a constant displacement of 0.7 cm for 5 minutes. Initially, the load decay was extremely rapid; afterwards, the load decayed at a much slower rate. Next, the response of the cervical spine to deformation rates of 0.127, 1.27, 12.7, and 64.0 cm/sec was determined. It can be seen from the results displayed in Figure 4.5 that the elasticity of the cervical spine, like other viscoelastic materials, is affected by the deformation history, along with the rate at which it is deformed.

The mechanical model chosen to represent the viscoelastic behavior of the neck in the ATB program consists of a spring in parallel with a dashpot (or damper), known as a Voigt body(6). The model, shown in Figure 4.6, takes into account passive resistance of the cervical spine, muscles and ligaments to axial deformation and angular displacement, but fails to consider the effects of active muscle contraction.

A linear spring produces a displacement proportional to
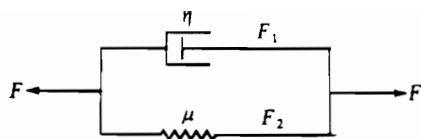
Figure 4.6   Voigt Body [6]

A fourth-order polynomial was used to fit the high rate initial loading curve of the relaxation test. The polynomial used was

$$F^e = 26 + 2600\delta - 5360\delta^2 + 18900\delta^3 - 14700\delta^4, \quad \delta < 0.76 \text{ cm}$$

MODEL CONSTANTS

$c = 0.331$

$\tau_1 = 0.003$ sec

$\tau_2 = 300.13$ sec

SOLID LINE - MODEL PREDICTIONS

MEASURED VALUES

x - 0.127 cm/sec

o - 1.27 cm/sec

* - 12.70 cm/sec

+ - 64.0 cm/sec
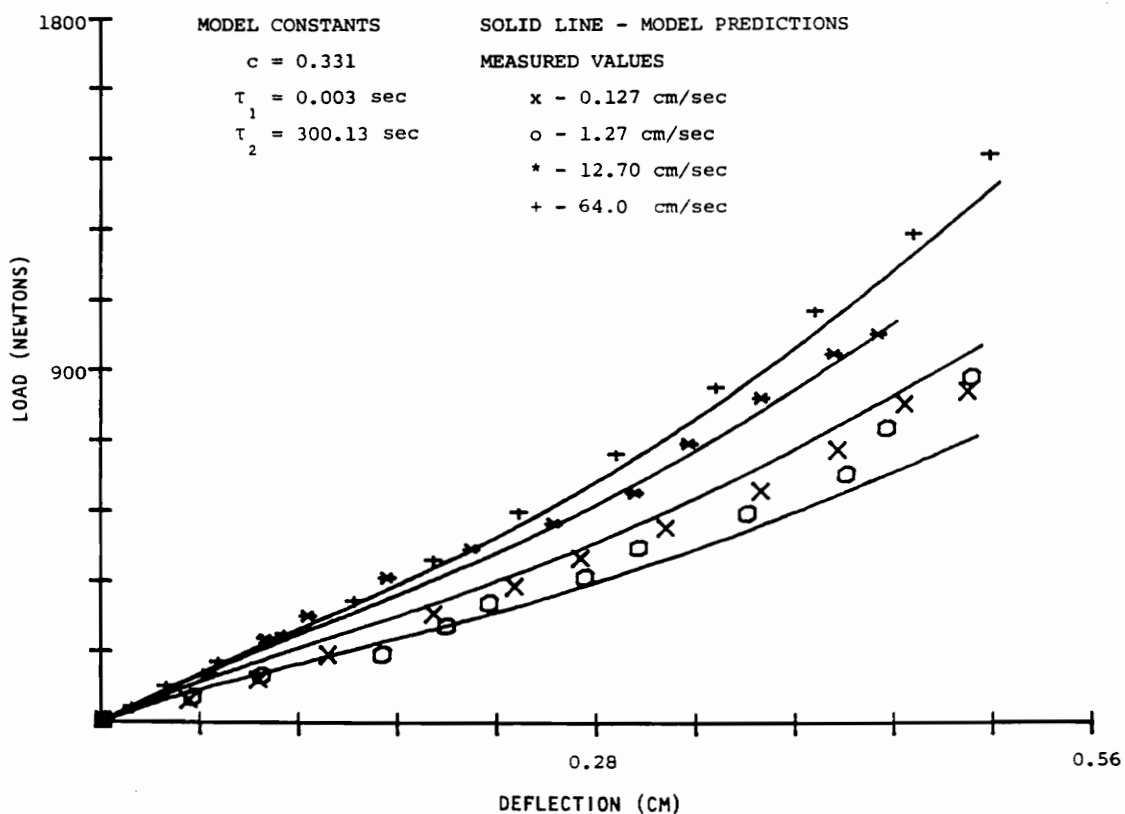
Figure 4.5   Response of Cervical Spine to Increasing Deformation Rates [7]

the force acting on the spring, while a dashpot produces a velocity proportional to the force. The spring and dashpot have the same displacement in a Voigt model. If x represents the linear displacement, $\dot{x}$ the velocity, and k and c are the spring constant and viscous coefficient, respectively, then the total force may be calculated as :

$$F = kx + c\dot{x} \qquad (4.1)$$

In the case of a torsional spring resisting angular displacement (flexion), x is replaced with the angle of rotation, θ, and $\dot{x}$ with $\dot{\theta}$.

In the present configuration of the ATB program, the spring and viscous coefficients are assigned initial values which remain constant throughout the entire simulation. Previous attempts were made to correlate simulations with experimental data for subject B9 in which several different combinations of values for these parameters were used. The ATB model allows the use of quadratic and cubic coefficients, which were also considered. The magnitude of the maximum head acceleration was reproduced within 98% of the target value, but the time at which it occurred was eight milliseconds past the actual measured maximum head acceleration.

Because of the complex nature of the neck, it follows

that the values of parameters governing the response of the neck model also change during the simulation. The present version of the ATB program does not allow parameters to vary with time. Therefore, the objective of this study is to modify the ATB program code to include time varying parameters in order to develop an adequate simulation. Resulting simulations will be compared with experimental data and previous simulations for subject B9. The validity of the ATB model will be based on its ability to reproduce the time and magnitude of the maximum z-direction head acceleration for subject B9.

5.0 METHODOLOGY

5.1 Development of NPs1 and c as Functions of Time

It was suggested that one unique set of viscoelastic parameters may not be sufficient for defining the subject's response throughout the entire simulation period; viscoelastic parameters are time-dependent and change in accordance with the deformation history of the material involved(11). The method chosen to verify this was to break the acceleration profile down into several different time periods, or phases, and to determine which values of k1, k2, c, NPs1 and NPv1 give the best simulated response for that phase(12). HPs1 and NPv1 were not included because the head pin was chosen to be locked, as mentioned previously. The goal of this method was to develop a regression equation that defines k1(t), k2(t), etc., instead of using finite sets of values for the parameters.

The experimental acceleration profile was broken down into four distinct phases: Phase I(0 $\leq$ t $\leq$ 45 msec), the Initial Impact Phase; Phase II(45 < t $\leq$ 95 msec), the Time-to-Peak Deceleration Phase; Phase III (95 < t $\leq$ 130 msec), the Neck Joint Attenuation (Plateau) Region; and Phase IV(130 < t $\leq$ 300 msec), the Final Period of Recovery(12). In order to match the simulated profile to the various phases of the experimental profile, all previous simulations

were reviewed, and portions of four simulations were chosen which provided the best fit for each phase. These simulations and four sets of values for k1, k2, c, NPs1 and NPv1 are shown in Figures 5.1A-D.

It was observed from these results that the linear spring coefficient, k1, along with the quadratic spring coefficient, k2, appeared to remain constant during the entire simulation period at values of 50 lb/in and 100 lb/in^2 , respectively. However, the linear damping coefficient, c, increased nearly four times in magnitude from a value of 1.5 to 5.6 lb-sec/in. The flexural characteristics of the neck/torso joint demonstrated the reverse behavior of the spring and damper, with the linear flexure damping coefficient, NPv1, remaining constant at 1.0 in-lb-sec/degree. The linear flexure spring coefficient, NPs1, decreased dramatically from an initial value of 880 in-lb/degree to a final value of 1.0 in-lb/degree. A suggested explanation for this drastic change in magnitude was that the subject may have initially braced himself in anticipation of the impact by actively contracting the muscles of his neck, eventually relaxing his muscles after impact(13).

As a result, a proposal was made to generalize the parameters c and NPs1 as functions of time in an effort to fit the experimental data using a single simulation. A
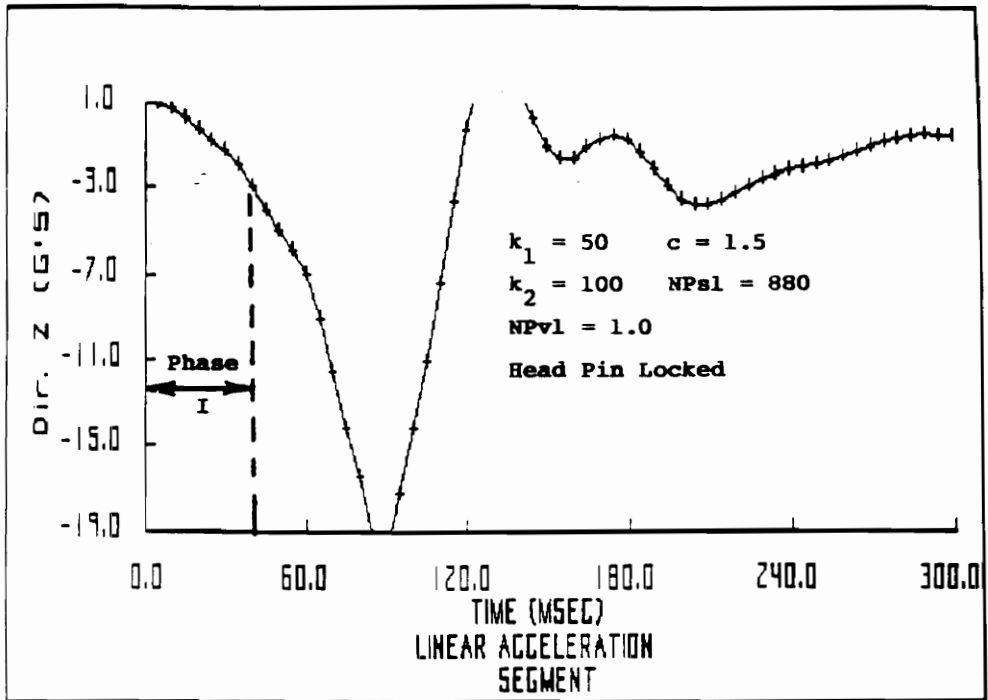
Figure 5.1A   Best-Fit Simulation for Phase I (12)
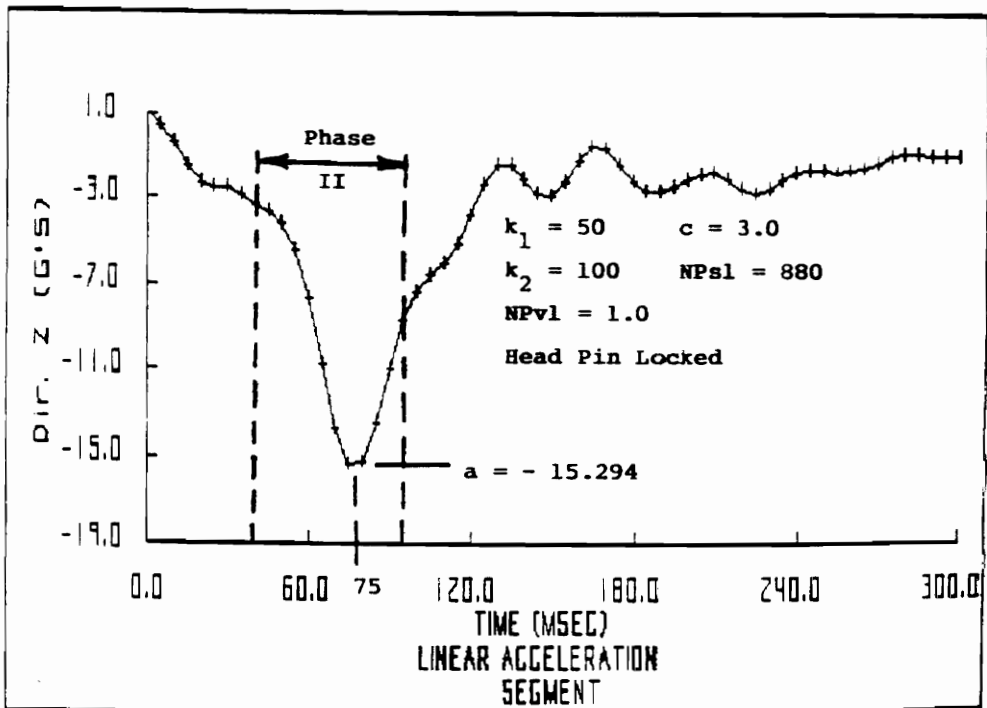
Figure 5.1B   Best-Fit Simulation for Phase II (12)

46
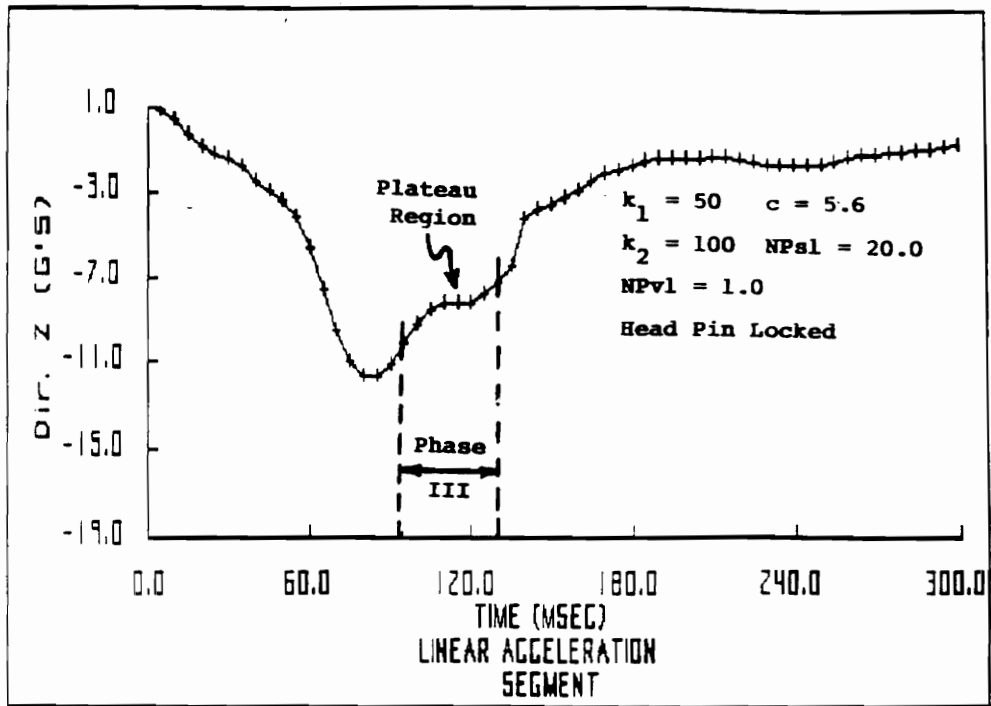
Figure 5.1C Best-Fit Simulation for Phase III (12)
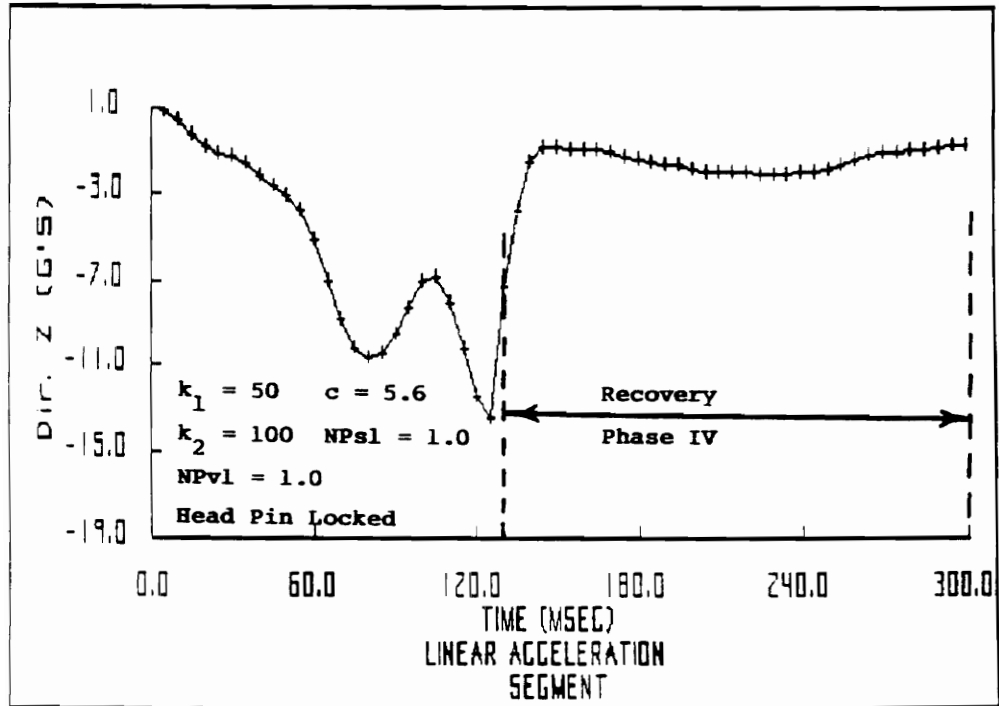
Figure 5.1D Best-Fit Simulation for Phase IV (12)

47

composite simulation, consisting of four pieces of different simulations which best fit the experimental data is shown in Figure 5.2. The maximum simulated head z-acceleration is equal to 16.3 G's, which is 94.1% of the actual measured head z-acceleration of 17.3 G's. There is a phase difference of 3 msec, with the measured maximum acceleration occurring before the simulated maximum acceleration.

Based on the values from these four simulations, functions of time describing $c(t)$ and $NPs1(t)$ were determined for subject B9. The linear viscous coefficient, $c(t)$, was determined to increase linearly with time up to 95 msec according to the equation(13):

$$c(t) = 0.043t + 1.5 \qquad t \leq 95 \text{ msec} \qquad (5.1)$$
$$c(t) = 5.6 \qquad t > 95 \text{ msec} \qquad (5.2)$$

After 95 msec, $c(t)$ remained constant at 5.6 lb-sec/in for the rest of the simulation. The linear flexure spring coefficient, $NPs1$, remained constant at 880 in-lb/degree up to 95 msec, after which it decreased exponentially according to the equation(13):

$$NPs1(t) = 879e^{-0.767(t-95)} + 1 \qquad (5.3)$$

The remaining values of $k1$, $k2$, and $NPv1$ are as described previously.
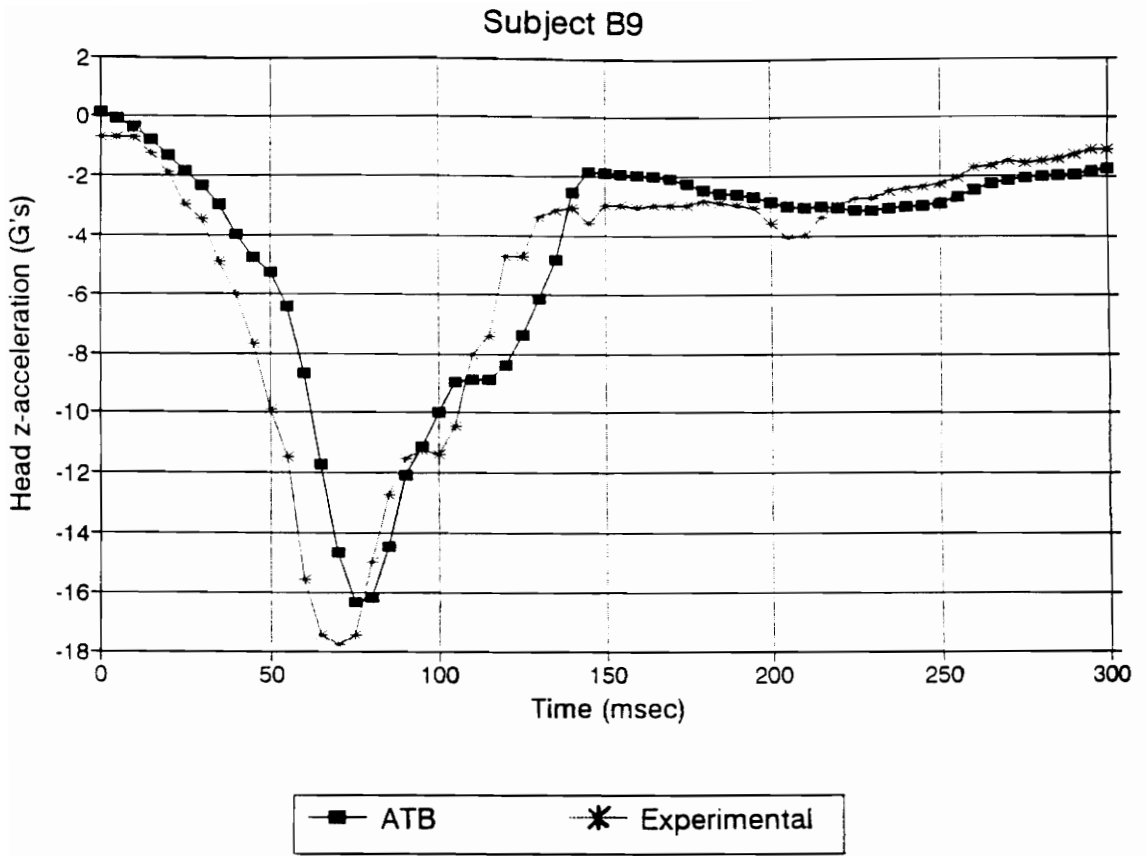
Figure 5.2 Composite Simulation Combining Four Best-Fit Simulations for Subject B9 (12)

5.2   Modifications to the ATB Program

The ATB program code was modified to include the linear viscous coefficient, c, and the linear flexure spring coefficient, NPs1, as functions of time c(t) and NPs1(t) described in section 5.1.   Previously, the ATB program did not allow time-varying parameters, and all parameters remained constant during simulations.   Two new subroutines listed in Appendix A, SPDNECK and SPDNECK2, were written and introduced into the program in which the values of c(t) and NPs1(t) are calculated, respectively.   Subroutine SPDNECK is called from subroutine SPDAMP, listed in Appendix B.   SPDAMP is called for each time increment and calculates the values of the spring and damper forces.   Subroutine SPDNECK2 is called from subroutine VISPR, listed in Appendix B. Subroutine VISPR is responsible for calculating the viscous and spring torques at the joints and is also called for each time increment.

Simulations using the modified ATB program were compared with the experimentally measured z-direction head acceleration profile for subject B9, which was chosen because 99.8% of the maximum resultant head acceleration occurred in the z-direction.   The output of the ATB program corresponds to an accelerometer with an initial setting of 0 G's, so that the simulated acceleration values are with respect to gravity, instead of absolute values.   The

experimental data has been adjusted accordingly, so that the maximum z-direction head acceleration is equal to 17.32 G's with respect to gravity. Emphasis was placed on the ability of the ATB model to reproduce this maximum acceleration because of the importance of predicting neck loads. The time-to-peak acceleration was also considered, along with the overall shape of the profile.

**Table 5.1 Initital Parameter Values For Subject B9
After Modifying Program**

NPs1	in-lb/deg	Eqn. 5.3
NPv1	in-lb-sec/deg	1.0
k1	lb/in	50
k2	lb/in^2	100
c	lb-sec/in	Eqn. 5.1

6.0   RESULTS

The initial head z-direction acceleration profile obtained after including c(t) and NPs1(t) are compared with the experimental head z-acceleration profile for subject B9 in Figure 6.1A. The values of parameters used in this simulation are listed in Table 5.1. For the simulated acceleration profile, the maximum acceleration of 17.53 G's occurs at 83 msec, 11 msec later than the measured maximum acceleration of 17.32 G's. The overall shape of the simulated profile has been improved, but the maximum amplitude has been exceeded, and the difference in time-to-peak acceleration values is actually greater than in previous simulations. Miller was able to obtain a maximum acceleration of 17.03 G's occurring at 80 msec (Figure 4.4).

In previous work, the viscous coefficients were found to affect the time-to-peak acceleration. As a result, a quadratic viscous coefficient, c2, was added to the spring and damper in an attempt to decrease the value of 83 msec. Several simulations were run using different values for c2, with a value of 1.5 lb-sec/in giving the best results. The addition of c2 shifted the time-to-peak acceleration to 77 msec, but resulted in a smaller magnitude of 16.73 G's, as shown in Figure 6.1B. Although the time of maximum acceleration has been improved, it is important to duplicate
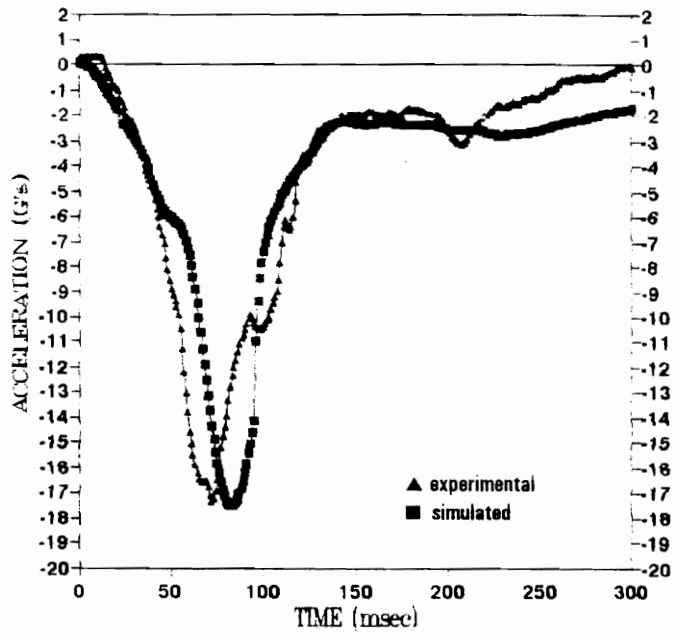
Figure 6.1A Simulated vs. Measured Z-Direction Head Acceleration
Profile Using Modified ATB Program

Figure 6.1B Simulated vs. Measured Z-Direction Head Acceleration
Profile Using Modified ATB Program With the Addition
of Quadratic Damping Coefficient

the magnitude of the head acceleration when predicting neck loads.

The value of the quadratic spring coefficient, k2, was increased in an attempt to increase the stiffness of the neck model rapidly with deformation. It was hoped that this would result in a greater impact of the head against the neck and higher values of acceleration. As expected, the maximum acceleration increased with increasing values of the quadratic spring coefficient, until a value of 17.30 G's was reached with k2 equal to 1800 lb/in^2. The time-to-peak acceleration shifted slightly to 78 msec. The resulting acceleration profile is shown in Figure 6.2; no further attempts were made to improve the simulation. When compared with the measured z-direction head acceleration profile for subject B9, the ATB model was able to duplicate the maximum acceleration, with an 8.3% difference in the time-to-peak acceleration values.
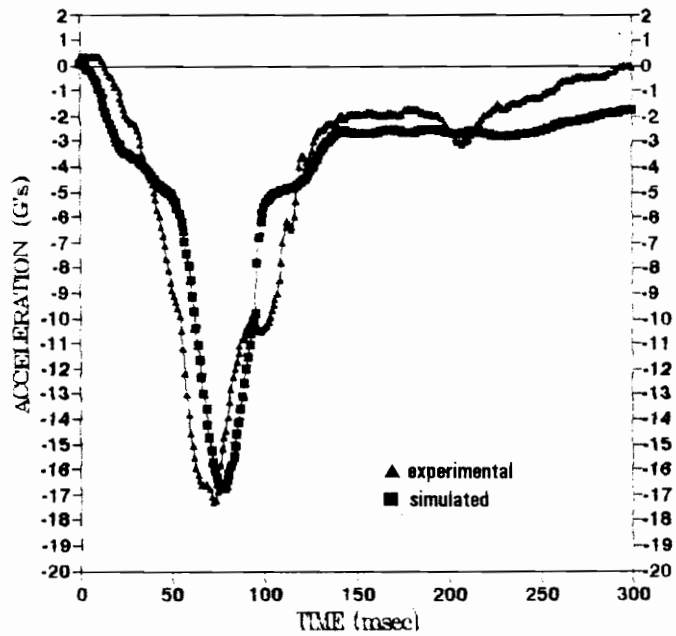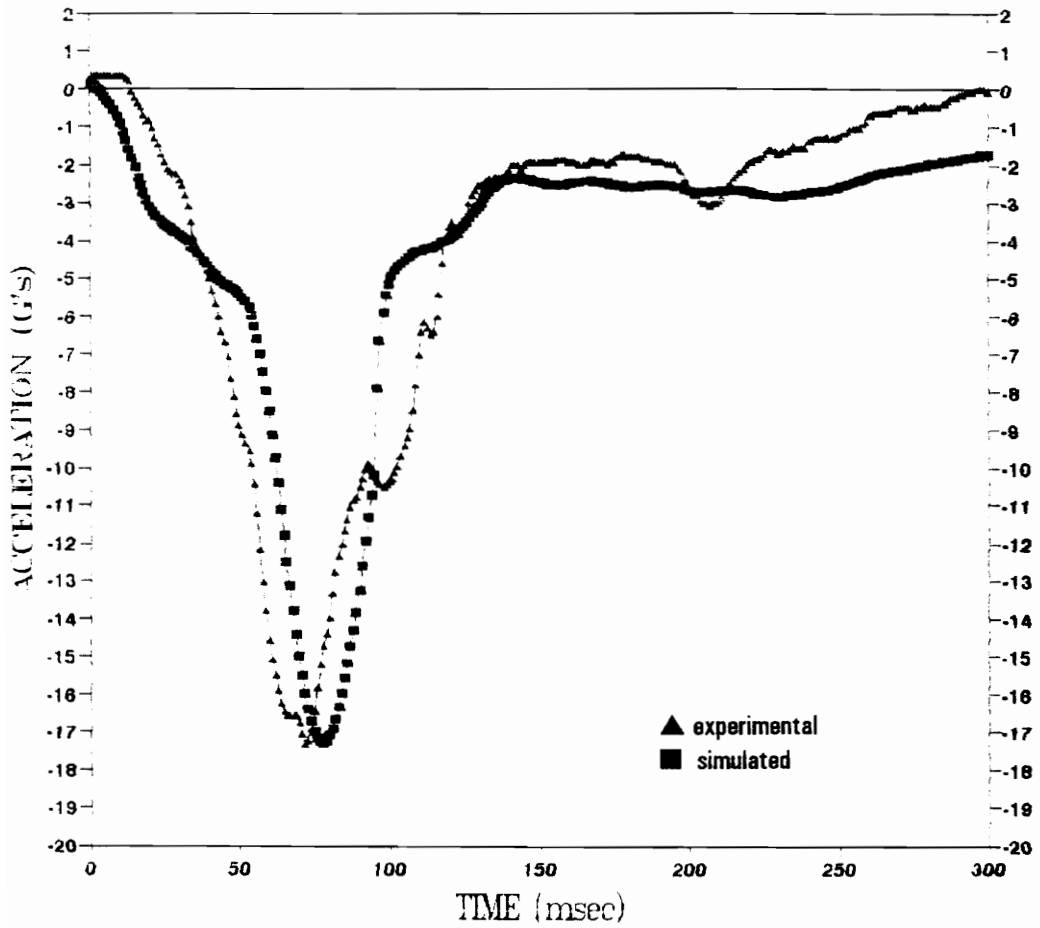
Figure 6.2   Simulated vs. Measured Z-Direction Head Acceleration
Profile Using Modified ATB Program With Increased Quadratic
Spring Coefficient

7.0 SUMMARY AND CONCLUSION

The ATB model was modified to include the linear flexure spring coefficient, NPs1, and the linear damping coefficient, c, at the neck/torso joint as functions of time for subject B9. Two new subroutines were introduced into the program in which NPs1(t) and c(t) are calculated for each time increment. Previously, an attempt was made to duplicate the experimentally measured head z-direction acceleration profile for subject B9 using the three segment representation of the head, neck, and upper torso. The head/neck joint was represented as a ball and socket joint, while the neck/torso joint was represented as a viscoelastic slip joint. A single set of parameters describing the response of the head and neck was not sufficient to reproduce the overall shape of the profile, although portions of the experimental response could be reproduced more accurately using different sets of parameter values. This led to the suggestion that some of the parameters should be represented as functions of time in order to adequately simulate the complex viscoelastic behavior of the neck.

The two parameters c and NPs1 were found to be linear and exponential functions of time, respectively, while the values of the other parameters remained relatively constant.

Initial simulations using the modified ATB model demonstrated an improvement in the maximum acceleration and overall profile of the response, with differences in the time-to-peak acceleration. A quadratic damping coefficient was introduced, and the quadratic spring coefficient was increased with good results. The maximum value of acceleration was duplicated, with only small differences in time-to-peak acceleration. This represented a small but measurable improvement over simulations using a constant set of parameter values, and suggested the direction in which future ATB-improvements should be headed.

The functions of time describing NPs1 and c were not intended to be precise; they are simple functions describing general changes in these parameters. It is possible that these parameters are more complex functions of time and that values of other parameters should also change during the simulation. The use of a program which could optimize values of the parameters would be helpful in determining this. The initially high value of NPs1, which decreases exponentially with time, suggests that the subject may have actively contracted the muscles in his neck in anticipation of impact. The addition of an element modeling active muscle contraction would improve the ability of the ATB model to simulate live human response.

The Voigt body may be too simplified to represent the

complex mechanical behavior of the neck. There is no method of determining the values of k1, k2, c1, c2, etc., for different subjects, and it is difficult to correlate these parameters with mechanical properties of the neck. The response of the head and neck to an axial impact and the mechanical properties of the neck must be more completely understood before an adequate model can be developed.

8.0 REFERENCES

1. Barineau, Daniel W., Schneck Daniel J. Improvements in the Control of Robotic Motion Simulations Using the ATB Model. Virginia Polytechnic Institute and State University Technical Report No. VPI-E-88-38, 1988.

2. Baugh, Donna Jo, Spittle, Eric K., Shipley, Buford W. "A New Technique For Evaluating The Dynamic Response of Head-Neck Systems To Helmets and Helmet Mounted Devices." Proceedings of the SAFE 30th Annual Symposium, Nov.2-4, 1992, pp.18-24.

3. Burham, John R. "A Comparison of Manikin and Human Dynamic Response to +Gz Impact." Proceedings of the SAFE 29th Annual Symposium, Nov.11-13, 1991, pp.32-35.

4. Estep, Christina R., Schneck, Daniel J. Modeling of the Human Head/Neck System Using Rigid Body Dynamics. Virginia Polytechnic Institute and State University Technical Report No. VPI-E-92-18, 1992.

5. Kaleps, Ints. "Prediction of Whole-Body Response to Impact Forces in Flight Environments." AGARD Conference Proceedings No.253, 1978, pp.A1-14

6. Fung, Y.C. Biomechanics: Mechanical Properties of Living Tissues, Second Edition. Springer-Verlag, NY, 1993.

7. McElhaney, James H., Paver, Jacqueline G., McCrackin, Hugh J., Maxwell, G. "Cervical Spine Compression Responses" Biomechanics of Impact Injury and Injury Tolerances of The Head-Neck Complex. Society of Automotive Engineers, Inc, 1993.

8. Miller, Heather L., Schneck, Daniel J. Biodynamic Responses to Emergency Ejections Under Conditions of Added Head Mass. Virginia Polytechnic Institute and State University Technical Report No. VPI-E-93-08, 1993.

9. Obergefell, Louise, Kaleps, Ints. "Modeling Human Body Dynamic Response to Abrupt Acceleration." Proceedings of the SAFE 31st Annual Symposium, Nov.8-10, 1993, pp.341-346.

10. Obergefell, L.A., Gardner, T.R., Kaleps, I., Fleck, J.T. Articulated Total Body Model Enhancements, Vol.2. Armstrong Laboratory Technical Report No. AAMRL-TR-88-043, Wright Patterson AFB, OH., 1988.

11. Schneck, Daniel J. "Biodynamic Responses to Emergency Ejections Under Conditions of Added Head Mass." Status Report, Aug.18, 1993.

12. Schneck, Daniel J. "Biodynamic Responses to Emergency Ejections Under Conditions of Added Head Mass." Status Report, Sep.15, 1993.

13. Schneck, Daniel J. "Biodynamic Responses to Emergency Ejections Under Conditions of Added Head Mass." Status Report, Oct.13, 1993.

14. Thornton, Jeffrey M. "An Improved Method for Determining the Mass Properties of Helmets and Helmet Mounted Devices." Proceedings of the SAFE 29th Annual Symposium, Nov.11-13, 1991, pp.87-93.

15. White, Richard P. Jr. "ADAM-The Physical Being." Proceedings of the SAFE 25th Annual Symposium, Nov.16-19, 1987, pp.141-149.

16. White, Richard P. Jr., Murphy, Brian P. "Development of a Mechanical Analog of a Human Spine And Viscera." Proceedings of the SAFE 23rd Annual Symposium, Dec. 1-5, 1985, pp.201-209.

17. Yoganandan, Narayan, Myklebust, Joel B., Ray, Gautam, Sances, Anthony Jr. "Mathematical and Finite Element Analysis of Spine Injuries." CRC Critical Reviews in Biomedical Engineering, Vol.15, Issue 1, 1987, pp.29-93.

APPENDIX A

New Subroutines Introduced Into The ATB Program

Subroutine SPDNECK, where c(t) is calculated:

```
*******************************************************************************
      SUBROUTINE SPDNECK(TIME,ASD)
      IMPLICIT REAL*8(A-H,O-Z)

      XM = 0.043
      B = 1.50
      TNOT =   0.095
      TEND =   0.300
      TN = TNOT*1000.0
      TM = TIME*1000.0

      IF (TIME.LE.TNOT) THEN
            ASD = XM*TM + B
            ELSE
            ASD = XM*TN + B
      END IF

      RETURN
      END
*******************************************************************************
```

Subroutine SPDNECK2, where NPs1(t) is calculated:

```
*******************************************************************************

      SUBROUTINE SPDNECK2(TIME,SPRING)
      IMPLICIT REAL*8(A-H,O-Z)

      TNOT =   0.095
      A = 879.0
      XN = -0.767
      TN = TNOT*1000.0
      TM = TIME*1000.0

      IF (TIME.LE.TNOT) THEN
            SPRING = A+1.0
            ELSE
            SPRING = A*(DEXP(XN*(TM-N)))+1.0
      END IF

      RETURN
      END
*******************************************************************************
```

APPENDIX B

Portion of Subroutine SPDAMP Where Subroutine SPDNECK Is Called

```
C       COMPUTE SPRING AND VISCOUS FORCE AND THE COMPONENTS              SPDAMP
C       ALONG THE UNIT VECTOR                                           SPDAMP
C                                                                       SPDAMP
        FS = 0.0                                                        SPDAMP
        FD = 0.0                                                        SPDAMP
        IF (ASD(1,I).LT.0.0) GO TO 21                                   SLIP
        DDO = DEL-ASD(1,I)                                              SPDAMP
        IF (DDO.LE.0.0 .AND. ASD(2,I).LE.0.0) GO TO 41                  SPDAMP
        CALL SPDNECK(TIME,ASD(4,I))                                          .
        FS = DDO*(DABS(ASD(2,I)) + DABS(DDO)*ASD(3,I))                  SPDAMP
        FD = DMV*(ASD(4,I)+DABS(DMV)*ASD(5,I))                          SPDAMP
        GO TO 29                                                        SPDAMP
     21 DDO = DEL+ASD(1,I)                                              SPDAMP
        JF1 = ASD(2,I)                                                  SPDAMP
        IF (JF1.EQ.0) GO TO 22                                          SPDAMP
        JF2 = NTI(JF1)                                                  SPDAMP
        IF (DDO.GT.0.0 .OR. ASD(3,I).EQ.0.0) FS = EVALFD(DDO,JF2,1)     SPDAMP
     22 JF3 = ASD(4,I)                                                  SPDAMP
        IF (JF3.EQ.0) GO TO 29                                          SPDAMP
```
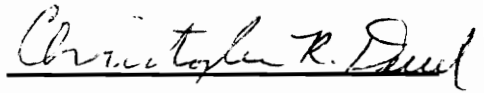
Portion of Subroutine VISPR where SPDNECK2 Is Called

```
C    COMPUTE CV, THE MAGNITUDE OF VISCOUS AND COULOMB TORQUE/WIJM       VISPR
C       RA = +SGN TA DOT = -WIJ.T7                                      VISPR
C      AND CSA, THE MAGNITUDE OF FLEXURE TORQUE/HAC                     VISPR
C                                                                       VISPR
     IF (J.EQ.1) THEN
        CALL SPDNECK2(TIME,SPRING(1,1))
     END IF
     CV = VISCOS(WIJM,VISC(1,3*J-2),HA2)                                VISPR
     IF (NJ.EQ.0) HA(2,2*J) = HA2                                       VISPR
     CREST = VISC(7,3*J-2)                                              VISPR
     RA = -(WIJ(1)*T7(1) + WIJ(2)*T7(2) + WIJ(3)*T7(3))                 VISPR
     IF (HAC.LT.EPS(12)) RA=0.0                                         MISDOT
     IF (HAC.GE.EPS(12)) RA=RA/HAC                                      MISDOT
     JSTP = 0                                                           VISPR
     IF (IPIN(J).EQ.7) GOTO 25                                          SLIP
     IF (JOINTF(J).EQ.0) CSA = EFUNCT(ANGL(1),RA,SPRING(1,3*J-2),JSTP)  VISPR
     IF (JOINTF(J).NE.0) CSA = FNTERP(ANGL(1),ANGL(2),JOINTF(J))        VISPR
     IF (HAC.LT.EPS(12)) CSA=0.0                                        MISDOT
     IF (HAC.GE.EPS(12)) CSA=CSA/HAC                                    MISDOT
  25 IF (NJ.EQ.0) JSTOP(1,1,J) = JSTP                                   SLIP
```

VITA

Christopher Deuel was born on September 5, 1969 in Berkeley, California, and later moved with his parents to Raleigh, N.C. in 1972. He received his high school diploma from Sanderson High School in Raleigh, and studied Mechanical Engineering at North Carolina State University in Raleigh, where he received his Bachelor of Science degree in December, 1991. He continued his studies at Virginia Polytechnic Institute and State University in Blacksburg, Virginia, in the Department of Engineering Science and Mechanics. He graduated with a Master of Science degree in Engineering Mechanics in June, 1994, with a specialization in Biomedical Engineering.

Christopher R. Deuel